Title

Implications of Future Price Trends and Interannual Resource Uncertainty on Firm Solar Power Delivery With Photovoltaic Overbuilding and Battery Storage

Journal

IEEE Transactions on Sustainable Energy, 14(4)

ISSN

1949-3029

Authors

Yang, Guoming

Yang, Dazhi

Lyu, Chao

et al.

Publication Date

2023

DOI

10.1109/tste.2023.3274109

Implications of Future Price Trends and Interannual Resource Uncertainty on Firm Solar Power Delivery with Photovoltaic Overbuilding and Battery Storage

Guoming Yang, Dazhi Yang, Chao Lyu, Wenting Wang, Nantian Huang, Jan Kleissl, Marc J. Perez, Richard Perez, and Dipti Srinivasan

***Abstract*—Generation from solar is inherently variable. Through a strategic combination of excessive capacity expansion (i.e., overbuilding) and battery storage, the variable solar generation can be cost-effectively firmed up, in that, it is able to meet the required generation target with absolute certainty. Firming up solar generation implies additional cost, which can be quantified through the firm kWh premium. This paper proposes a new model for the optimization of firm kWh premium through either a mixed-integer linear program or a bilinear program, depending on whether a generic or detailed battery model is used. The (bi)linear-program formulation greatly reduces the complexity of the original iterative approach. Additionally, since the firm kWh premium is a function of photovoltaic and battery prices, we show how future price change can affect the economics of firm power delivery and whether true grid parity can be eventually achieved. Lastly, the sensitivity of the firm kWh premium to photovoltaic modeling uncertainty and inter-annual solar resource uncertainty is analyzed.**

***Index Terms*—Firm power delivery, Firm kWh premium, Photovoltaic, Battery storage.**

NOMENCLATURE

Indexes

i, o	Indexes of the sets of charging/discharging measurement data $\mathcal{I}$ and $\mathcal{O}$
t	Index of time-period set $\mathcal{T}$

Parameters

B_h	Beam horizontal irradiance
B_n	Beam normal irradiance
c_b, c_s	Unit investment costs of battery storage and PV plant
D_h	Diffuse horizontal irradiance
F_1, F_2	Sky-condition-dependent parameters of the Perez model
G_c	Global tilted irradiance
G_h	Global horizontal irradiance
l_b, l_s	O&M cost factor of battery storage/PV plant
$N_{\text{max},\,b}$	Upper bound of N_b
$N_{\text{min},\,b}$	Lower bound of N_b
P_{ac}, P_{dc}	AC and DC power output of the PV plant
$P_{\text{ac,ref}}$	AC power output limit of the inverter
$P_{\text{ch,max}}$	Maximum charging power of battery
$P_{\text{dc,ref}}$	DC power input limit of the inverter
$P_{\text{dis,max}}$	Maximum discharging power of battery
$P_{\text{load},\,t}$	Load demand at time t
$P_{\text{PV},\,t}$	PV power output
P_s	Original rated power of PV plant
R_d	Diffuse transposition factor
R_r	Transposition factor due to ground reflection
S	Tilt angle of PV surface
$S_{b,\,\text{ref}}$	Nameplate capacity of the battery that is used to obtain the sample data
T_{amb}	Ambient temperature
T_b, T_s	Lifetimes of battery storage and PV plant
T_{cel}, T_{mod}	Cell and module temperatures
Z	Solar zenith angle
ε_b	Battery charging/discharging efficiency
ζ	Convergence tolerance of bisection algorithm
η_{inv}	Actual inverter efficiency
η_{norm}, η_{ref}	Nominal and reference inverter efficiencies
γ_{ref}	Temperature coefficient of the rated power of the PV modules
ρ	Foreground's albedo
σ_b	Battery self-discharge rate
τ	Discount rate
θ	Incidence angle
ξ_b, ξ_s	Capital recovery factors of battery and PV plant
Δt	Unit time interval
ΔT, p, q	Empirical coefficient of the Sandia model

Variables

b_1, b_2	Model status in the bisection algorithm
$B_{\text{ch},\,t}$, $B_{\text{dis},\,t}$	Binary variables denoting the charging/discharging mode of battery storage
$E_{b,\,1}$	Available energy of battery storage during time $t = 1$

(Corresponding author: Dazhi Yang) G. Yang, D. Yang, C. Lyu, W. Wang are with the Department of Electrical Engineering and Automation, Harbin Institute of Technology, Harbin, Heilongjiang, China (email: yangguoming1995@gmail.com; yangdazhi.nus@gmail.com; lu_chao@hit.edu.cn; wangwenting3000@gmail.com). N. Huang is with the Key Laboratory of Modern Power System Simulation and Control & Renewable Energy Technology (Northeast Electric Power University), Ministry of Education, Jilin, Jilin, China (email: huangnantian@126.com). J. Kleissl is with the Center for Energy Research, Department of Mechanical and Aerospace Engineering, University of California, San Diego, CA, USA (email: jkleissl@eng.ucsd.edu). M.J. Perez is with Clean Power Research, Napa, CA, USA (email: marc.j.r.perez@gmail.com). R. Perez is with the Atmospheric Sciences Research Center, University at Albany, SUNY, Albany, NY, USA (email: solarperez@gmail.com). D. Srinivasan is with the Department of Electrical and Computer Engineering, National University of Singapore, Singapore (email: dipti@nus.edu.sg).

$E_{b,\,t}$, $E_{b,\,t+1}$	Available energy of battery storage at t and $t+1$
N_b	Integer number of batteries in relation to the battery with a rated capacity of $S_{b,\,\text{ref}}$
N_b^*	Optimal battery number in the bilinear model
N_{mid}	Auxiliary variable in the bisection algorithm
$P_{\text{ch},\,t}$, $P_{\text{dis},\,t}$	Charging and discharging power of battery storage
$P_{\text{curt},\,t}$	Curtailed power of PV plant
$P_{\text{grid},\,t}$	PV power directly injected to the grid
$P_{\text{in},\,t}$	Power fed into the battery after the charging efficiency has been considered
$P_{\text{out},\,t}$	Power output from the battery before the discharging efficiency has been considered
S_b	Rated capacity of battery storage
SoC_t	State of charge of the battery
X_s	Oversizing ratio of the PV plant
$x_{i,\,t}$, $x_{o,\,t}$	Related to the choice of the charging or discharging measurement data
y_1, y_2	Objective function values in the bisection algorithm
$\eta_{\text{ch},\,t}$, $\eta_{\text{dis},\,t}$	Charging and discharging efficiencies of the battery storage

I. Introduction

RENEWABLES, such as wind or solar, differ from conventional generation by their variable and uncertain nature, in that, they are not dispatchable. To tame such variability and uncertainty, electric storage [1, 2], geographical smoothing [3, 4], and demand response [5, 6] are common technologies, which have hitherto been frontiers of energy research. As these technologies all seek to firm up the renewable generation, they can be grouped under the umbrella term of *firm power enablers* [7]. The phrase "firm power" refers to the kind of power from renewables that is able to meet the required generation target, may it be the load demand or the forecast generation amount, with 100% certainty. Hence, one may interpret firming up renewable generation as a means of turning non-dispatchable power to dispatchable power.

In a nutshell, all aforementioned firm power enablers alter the generation and load profiles, so as to facilitate the balancing between the two on a variety of spatial and temporal scales, which is a problem concerning power system operations at large. Taking for instance electric storage, its fundamental operating principle is to store energy when there is a surplus of renewable generation, and to release the stored energy when there is a deficit. Stated differently, the role of electric storage is to shift the generation peaks so as to match the demand peaks. The operating principles of geographical smoothing and load shaping are similar, with the former aims at modifying generation and the latter load.

Nonetheless, each firm power enabler, while being attractive in its own respect, has disadvantages that can be easily thought of. Batteries are at present costly. Particularly during the prolonged periods of energy deficit, such as nighttime or winter when there is no solar, the required storage capacity to firm up the generation could be exceedingly high. Under the current market economics and remuneration frameworks, that is simply not financially viable. Geographical smoothing, on the other hand, is passive in nature, as it depends for its success upon the size and spatial distribution of installed renewable energy farms, which are not in the system operators' control. Last but not least, load shaping requires the coordination and compliance of individual consumers, who are advised to change their electricity consumption behavior, which is known *a priori* difficult.

In view of the drawbacks of these existing firm power enablers, another somewhat counter-intuitive technology has been proposed very recently, that is, overbuilding & proactive curtailment [8]. The idea central to this enabler is to elevate the generation profile by expanding the capacity of a plant, such that most variations in power output take place above the load profile. Certainly, overbuilding leads to energy excess, which is to be either stored or proactively curtailed. On appearance, curtailment is contradictory to the conventional wisdom of energy utilization, and thus should be minimized. But in fact, as shown by Perez et al. [8], this counter-intuitive firm power enabler constitutes an attractive alternative of electric storage; for that reason, the overbuilt part is known as *implicit storage* [9]. The concept of overbuilding & proactive curtailment is elaborated in Fig. 1, in which the daily energy generation profiles of both the unconstrained (i.e, "business-as-usual" installation without battery and overbuilding) and 2x overbuilt versions of a 1-MW photovoltaic (PV) system are plotted with respect to the daily energy consumption of a 0.17-MW constant load (assumed here for simplicity). For the unconstrained PV plant, i.e., no PV oversizing, much energy deficit is seen, which needs to be supplied through on-site electric storage or by other means, whereas for the overbuilt PV plant, the energy deficit is substantially reduced (although a much higher curtailment is now evident).

Through the above toy example, one can notice two things. First, if the variability of the PV production (herein used to exemplify renewable production) is to be fully resolved via a battery-only solution, the storage capacity requirement would be excessively high. Second, if the variability of the PV production is to be fully resolved via overbuilding, the overbuilding factor needs to be exceedingly large, such that even the lowest dip in generation still stays above the load demand. Clearly then, a combination of these two enablers is logically attractive. The technical problem of concern is therefore one of optimization, which endeavors to estimate the most cost-effective mix of explicit and implicit storage.

In the literature, firm solar power delivery has been discussed numerous times, but each time under a different scenario [8–12]. These previous works on firm power can be categorized into two modes, one deals with *firm forecasting*, which takes storage and overbuilding as a means to remove the discrepancies between actual generation and forecast, the other deals with *firm generation*, which leverages the same enablers to remove the discrepancies between actual generation and load demand. As noted by Perez et al. [10], the difference between these two modes is only in scale, in that, firm forecasting represents an entry-level application of firm power, and firm generation depicts the ultimate ideal in which the

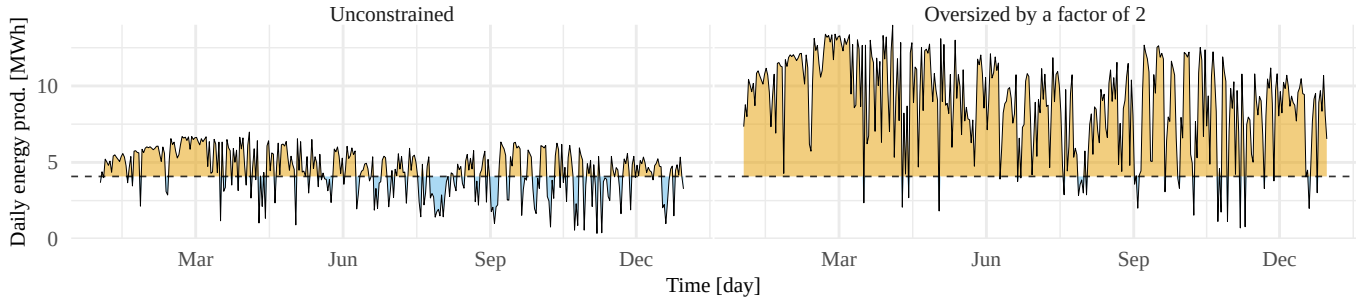

Fig. 1. (left) The daily energy production (black solid line) of a 1-MW PV system situated in Harbin, China, serving a 0.17-MW constant load (dashed line). PV energy calculation using the model chain is elaborated in Section III. Whereas the energy deficit (blue shade) needs to be fulfilled through battery storage, the surplus (orange shade) needs to be either stored or curtailed. (right) The same setup but with a PV oversizing factor of 2, showing much reduction in energy deficit, and thus much lower demand for batteries.

full load is satisfied by renewables alone, which is a much harder task. In delivering firm power in real life, various sources of uncertainty, such as the variable load and the suboptimal battery dispatch schedule, would trigger additional overbuilding requirements in the case of firm power delivery, but that should not concern the present study.

Although some preliminary investigations on firm power delivery have been conducted, the topic is still in its infancy, and there are many aspects of it that are still opaque. For example, the obtaining of the least-cost combination of storage and overbuilding has only been mathematically described in the original doctoral thesis from 2014 [12], but not in any subsequent paper. More importantly, the original approach involves two nonlinear optimization problems that estimate the oversizing ratio and storage capacity not only separately but also through direct search (Nelder–Mead method) and bisection (Brent method), which as numerical methods are inefficient. The technique, as a result, is difficult to reproduce from the extant literature alone. For that reason, we wish to formalize the procedure for acquiring the optimal *firm kWh premium*, which quantifies the overall cost-effectiveness of firm power generation. Next to that is the lack of in-depth analysis on the implication of prices of PV and battery on the optimization results. As prices of PV and battery are bound to drop in the the future, it is of interest to understand whether firm solar power can ever achieve true grid parity, or at least to have a ballpark figure on the price needed to achieve true grid parity. Another influencing factor is the choice of PV and battery models, which necessarily affects the optimization results. To that end, several PV *model chains* (a physical PV modeling framework) and two different battery models (one generic and the other detailed) should be considered and compared. Last but not least, since PV power is governed chiefly by the interplay of solar resource availability and electricity demand, one has to investigate the effects of inter-annual variability (or equivalently, uncertainty) in solar resource on firm power delivery.

To summarize, the contribution of this paper is three-fold: (1) we show for the first time that the optimization problem concerning firm power delivery can be written into a (bi)linear program, and a new algorithm for calculating the optimal firm kWh premium is thereby proposed; (2) the implications of future price trends of PV and battery on firm power generation are investigated through an eclectic mix of price scenarios; and (3) the uncertainty in determining the optimal firm kWh premium is quantified on two respects, of which one is the PV and battery physical modeling choice, and the other is the variability in inter-annual solar resource. The remaining part of the paper is organized as follows. Section II first discusses the logic rule governing the operation of a firm solar power plant. Then, it introduces the measure called firm kWh premium, as well as how to optimize it. Section III is attributed to model chain, which is a physical framework for modeling a PV plant, and is essential for plant siting, design, simulation, and performance evaluation. The sensitivity of the firm kWh premium to the choice of the model chain, prices of PV and battery, as well as to solar resource uncertainty, is analyzed in Section IV, through a case study. Conclusions follow at the end.

II. Logic Rule of Firm Power Delivery and Optimization of Firm kWh Premium

Unlike the unconstrained PV plant, the firm PV plant is configured with battery storage and a control system to dynamically limit the PV generation if necessary, namely, to store or curtail the excess solar power. In addition, the installed capacity of a firm PV plant is deliberately expanded to increase the probability of PV generation exceeding load demand.

A. Logic Rule and Cost-Effectiveness Measure of Firm Power

Figure 2 depicts the schematic diagram and flowchart of the operating principle of a firm PV plant. As can be seen from the figure, when PV generation is greater than load demand, excess energy is used to charge the battery. However, if the battery is full, that surplus of energy is curtailed. When PV generation is lower than load demand, the firm PV plant directly delivers all produced power to the load side, and the energy deficit is made up by battery storage. With these coordinated strategies, the firm PV plant can supply the system operators with a contracted amount of PV power, which could be either the supply of a local load such as a microgrid or a promised generation amount that is part of a larger power system. In other words, the generation target can be fully satisfied, on a 24x365 basis, by the firm PV plant, which,

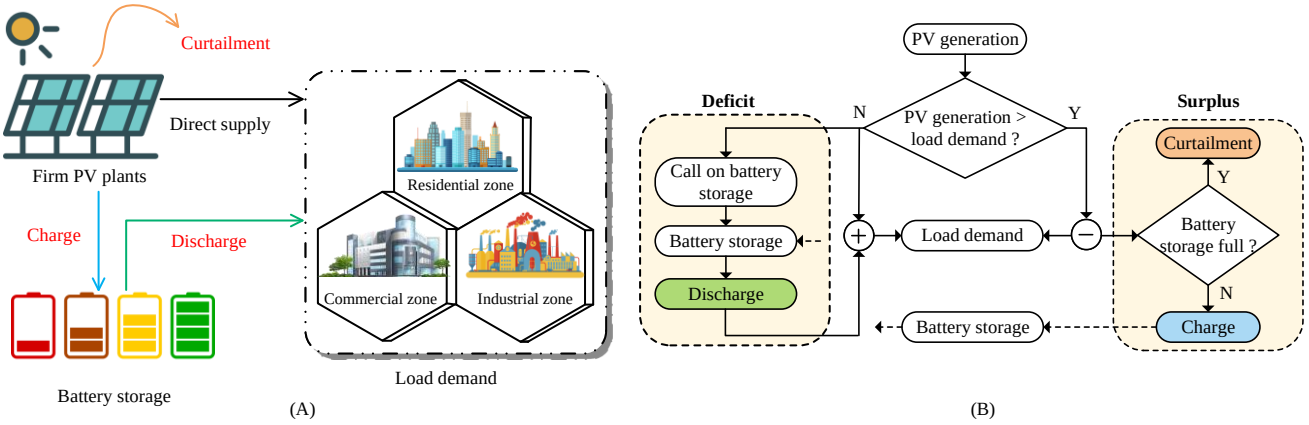

Fig. 2. (A) Schematic diagram and (B) flowchart showing the operating principle of a firm PV plant. When PV power exceeds load demand, solar energy surplus can be either charged or curtailed; when PV power is below load demand, the energy deficit is replenished by the battery storage.

just like conventional generators, can thus be regarded as dispatchable power sources.

To gauge the economics of firm PV generation, a measure called "firm kWh premium," which is closely related to the levelized cost of electricity (LCOE), is needed, and it takes the form:

$$\text{Firm kWh premium} = \frac{\text{Firm PV generation LCOE}}{\text{Unconstrained PV LCOE}}, \quad (1)$$

where

$$\text{LCOE} = \frac{\text{Equivalent annual cost of generation}}{\text{Equivalent annual electricity produced}}. \quad (2)$$

As revealed in Eq. (1), the firm kWh premium relates the LCOE of a firm PV plant to that of an unconstrained PV plant; it can be regarded as the cost multiplier to firm up PV generation. To compute LCOE using Eq. (2), one needs to collect three components: (1) the equivalent annual investment cost (CapEx), (2) equivalent annual operation and maintenance (O&M) cost (OpEx), and the equivalent annual electricity produced.

It should be noted that for unconstrained PV, the equivalent annual cost is simply the sum of CapEx and OpEx of PV, whereas for firm PV, its cost includes additional the CapEx and Opex of batteries. On the other hand, the equivalent annual electricity produced by unconstrained PV is just its generation amount, whereas that of firm PV is in fact the assigned generation target, for it needs to meet that target with absolute certainty. In summary, the two LCOEs involve four terms, among which three are fixed. The only variable term is the equivalent annual cost of firm PV.

B. Formulation of the Optimization Problem

The objective function consists of the equivalent annual investment cost and O&M cost of the PV plant and battery storage, which can be described as:

$$\underset{X_s, S_b, P_{\text{ch},\,t}}{\arg\min} \left\{ c_s X_s P_s \left(\xi_s + l_s\right) + c_b S_b \left(\xi_b + l_b \sum_{t=1}^{8760} \frac{P_{\text{ch},\,t}}{S_b} \right) \right\}, \quad (3)$$

with

$$\xi_s = \frac{\tau(1+\tau)^{T_s}}{(1+\tau)^{T_s}-1}, \quad \xi_b = \frac{\tau(1+\tau)^{T_b}}{(1+\tau)^{T_b}-1}, \quad (4)$$

where subscript s, abbreviated from the word "solar," denotes quantities relevant to PV; subscript b, abbreviated from the word "battery storage," denotes quantities relevant to battery storage; subscript t indexes time and takes value from the integer set $\{1, 2, \ldots, 8760\}$ representing hours in a year; ξ is the capital recovery factor; c is the investment cost per kW for PV plant or per kWh for battery storage; l is the O&M cost factor; T is the lifetime in units of years; X_s is the oversizing ratio of the PV plant; P_s is the original rated power in kW of the PV plant; S_b is the rated capacity in kWh of battery storage; $P_{\text{ch},\,t}$ is the charging power of battery storage, and τ is the discount rate.

The first term in Eq. (3) refers to the equivalent annual cost of PV, whereas the second term shows the equivalent annual cost of battery storage. Typically, the O&M cost of battery storage is approximated using the number of full charge cycles. In other words, l_b of the investment cost is assumed for the cost of a full charge cycle of battery storage. As expressed in Eq. (4), the capital recovery factors of the PV plant and battery storage are calculated from the discount rate and corresponding equipment lifetime.

During firm PV plant operation, some constraints must not be violated, which include the load demand constraint and the operation constraints of the PV plant and battery storage:

1) Load demand constraint: The PV plant and battery storage jointly meet the load demand. Mathematically,

$$P_{\text{load},\,t} = P_{\text{grid},\,t} + P_{\text{dis},\,t}, \ \forall t \in \mathcal{T}, \quad (5)$$

where $\mathcal{T}$ is the set of time periods; $P_{\text{load},\,t}$ is the load demand at time t; $P_{\text{grid},\,t}$ is the PV power directly injected to the grid; and $P_{\text{dis},\,t}$ is the discharging power. The equality constraint (5) indicates that load demand must be fulfilled at any instance t.

2) PV plant operation constraint: As shown in Fig. 2 (A), the energy balance of the PV plant is represented by the three arrows leaving the PV plant. Stated differently, PV power generated by the plant comprises three components:

(1) curtailed power, (2) power directly delivered to the load side, and (3) power to charge the battery. The relationship is expressed as:

$$P_{\text{PV},\,t} = P_{\text{curt},\,t} + P_{\text{grid},\,t} + P_{\text{ch},\,t},\ \forall t \in \mathcal{T}, \tag{6}$$

where $P_{\text{curt},\,t}$ is the curtailed power at time t, and $P_{\text{PV},\,t}$ is the PV power output, which can be acquired either by measurement or through simulation.

3) Battery storage operation constraints (battery model A): This paper considers and compares two battery models, one simple (this subsection) and one detailed (next subsection), as to investigate the effects of battery model on firm kWh premium calculation. The operation constraints of the generic battery storage model A are as follows:

$$0 \le P_{\text{ch},\,t} \le B_{\text{ch},\,t} P_{\text{ch,\,max}}, \tag{7}$$

$$0 \le P_{\text{dis},\,t} \le B_{\text{dis},\,t} P_{\text{dis,\,max}}, \tag{8}$$

$$B_{\text{ch},\,t} + B_{\text{dis},\,t} \le 1, \tag{9}$$

$$E_{b,\,t+1} = (1-\sigma_b)E_{b,\,t} + \Delta t \left(\varepsilon_b P_{\text{ch},\,t} - \frac{P_{\text{dis},\,t}}{\varepsilon_b}\right), \tag{10}$$

$$0 \le E_{b,\,t} \le S_b, \tag{11}$$

$$E_{b,\,1} = 0.8 S_b, \tag{12}$$

where $\forall t \in \mathcal{T}$ applies to all equations with t subscripts; $P_{\text{ch,\,max}}$ and $P_{\text{dis,\,max}}$ are the maximum charging and discharging power of battery storage, respectively; $B_{\text{ch},\,t}$ and $B_{\text{dis},\,t}$ are binary variables denoting the operation mode of the battery storage, in that, when $B_{\text{ch},\,t}$ or $B_{\text{dis},\,t}$ holds the value of 1, the corresponding mode is triggered, otherwise deactivated; $E_{b,\,1}$, $E_{b,\,t}$, and $E_{b,\,t+1}$ are the available energy in kWh of battery storage during time $t = 1$, t, and $t+1$, respectively; σ_b is the battery self-discharge rate; ε_b is the battery charging/discharging efficiency, and Δt is the unit time interval, which is 1 h in this case.

Constraints (7) and (8) require that the charging and discharging power of battery storage are lower than their related maximum values. Constraint (9) guarantees that no simultaneous charging and discharging mode can occur. The equality constraint (10) specifies the energy balance of the battery storage, that is, the available energy at each hour plus the charging power times the time step (or minus the discharging power) is equal to the stored energy at the next hour, while the self-discharge rate and charging/discharging efficiency are considered. Constraint (11) requires the available energy of the battery storage at any instance to be within its rated capacity. Last but not least, the initial stored energy of battery storage is set as 0.8 times the rated capacity, as shown in Eq. (12). The value of 0.8 in Eq. (12) is arbitrarily selected. Choosing a value too small may fail the optimization, as the first few hours/days in a year may correspond to no- or low-resource situations during which power has to be drawn from the battery, and some initial reserve is essential.

4) Battery storage operation constraints (battery model B): Since the generic battery model A may be deemed as overly ideal, which may leads to an over-confident battery utility, many detailed battery models have recently emerged to capture/reflect the real operation behaviors of the battery [13, 14]. To that end, a measurement-based battery storage model B, which was proposed by Gonzalez-Castellanos et al. [15] and has been applied to the energy dispatch optimization of a microgrid [16], is additionally considered in this work. This battery model leverages a sampling-based approach on the charging/discharging measurements to allow an accurate portrait of the working of the battery. Before further explanation, the meaning of some symbols is given first. $P_{\text{in},\,t}$ represents the power fed into the battery after the charging efficiency has been considered at time t, whereas $P_{\text{out},\,t}$ specifies the power output from the battery before the discharging efficiency has been considered at time t; SoC_t is the state of charge (SoC) of the battery at time t, which is defined as the ratio of available energy at that time to its rated capacity. Vector $\left(\widehat{\text{SoC}}_{\text{ch},\,i}, \widehat{P}_{\text{ch},\,i}, \widehat{P}_{\text{in},\,i}\right), i \in \mathcal{I}$, is the 3-dimensional representation of the battery charging measurements, whereas the discharging measurements are recorded as $\left(\widehat{\text{SoC}}_{\text{dis},\,o}, \widehat{P}_{\text{dis},\,o}, \widehat{P}_{\text{out},\,o}\right), o \in \mathcal{O}$. $\mathcal{I}$ and $\mathcal{O}$ are the sets of battery charging and discharging measurements, respectively. The main idea of this battery model is that the two sample sets are used to span the feasible region of battery operations. In other words, an arbitrary battery operation point $\left(\text{SoC}_t, P_{\text{ch},\,t}, P_{\text{in},\,t}\right)$ or $\left(\text{SoC}_t, P_{\text{dis},\,t}, P_{\text{out},\,t}\right)$ can be expressed as a convex combinations of the corresponding sample set.

Constraints of battery model B can be expressed as follows:

$$E_{b,\,t+1} = E_{b,\,t} + P_{\text{in},\,t}\Delta t - P_{\text{out},\,t}\Delta t, \tag{13}$$

$$P_{\text{in},\,t} = \sum_{i\in\mathcal{I}} x_{i,\,t} N_b \widehat{P}_{\text{in},\,i}, \tag{14}$$

$$P_{\text{ch},\,t} = \sum_{i\in\mathcal{I}} x_{i,\,t} N_b \widehat{P}_{\text{ch},\,i}, \tag{15}$$

$$P_{\text{out},\,t} = \sum_{o\in\mathcal{O}} x_{o,\,t} N_b \widehat{P}_{\text{out},\,o}, \tag{16}$$

$$P_{\text{dis},\,t} = \sum_{o\in\mathcal{O}} x_{o,\,t} N_b \widehat{P}_{\text{dis},\,o}, \tag{17}$$

$$\text{SoC}_t = \sum_{i\in\mathcal{I}} x_{i,\,t}\widehat{\text{SoC}}_{\text{ch},\,i} + \sum_{o\in\mathcal{O}} x_{o,\,t}\widehat{\text{SoC}}_{\text{dis},\,o}, \tag{18}$$

$$\sum_{i\in\mathcal{I}} x_{i,\,t} = 1,\ 0 \le x_{i,\,t} \le 1, \tag{19}$$

$$\sum_{o\in\mathcal{O}} x_{o,\,t} = 1,\ 0 \le x_{o,\,t} \le 1, \tag{20}$$

$$E_{b,\,t} = \text{SoC}_t S_b, \tag{21}$$

$$S_b = N_b S_{b,\,\text{ref}}, \tag{22}$$

$$0 \le N_b \le N_{\text{max},\,b}, \tag{23}$$

$$0 \le E_{b,\,t} \le S_b, \tag{24}$$

$$E_{b,\,1} = 0.8 S_b, \tag{25}$$

where $\forall t \in \mathcal{T}$ applies to all equations with t subscripts; $x_{i,\,t}$ is the weight assigned to the i^{th} charging measurements, which decides a specific battery charging point, and is to be determined by the optimization. Similarly, $x_{o,\,t}$ is the weight assigned to the o^{th} discharging measurements. $S_{b,\,\text{ref}}$ is the nameplate capacity of a unit of battery of concern, which was used to obtain the sample measurements. Here, the obtained battery parameters are assumed to be linearly scalable to any capacity of the battery, thus N_b indicates the integer number

of batteries that are installed in the firm PV plant. In addition, $N_{\text{max},\,b}$ is the upper bound of N_b.

Two aspects separate battery model B from battery model A: (1) in model B, the maximum charging power and maximum discharging power depend upon the available energy in the battery; and (2) in model B, the battery charging efficiency ($\eta_{\text{ch},\,t}$) and discharging efficiency ($\eta_{\text{dis},\,t}$) are time-varying. The former aspect is due to the fact that Eqs. (14–15, 18–19) limit the feasible region of $\left(\text{SoC}_t, P_{\text{ch},\,t}, P_{\text{in},\,t}\right)$ using the charging measurements, and similarly Eqs. (16–18, 20) limit the feasible region of $\left(\text{SoC}_t, P_{\text{dis},\,t}, P_{\text{out},\,t}\right)$ using the discharging measurements. Since the efficiencies of the battery are defined as $\eta_{\text{ch},\,t} = P_{\text{in},\,t}/P_{\text{ch},\,t}$ and $\eta_{\text{dis},\,t} = P_{\text{dis},\,t}/P_{\text{out},\,t}$, they are implicitly built into the model. This model not only captures the time-varying nature of the charging/discharging efficiencies, and it further allows a linear energy balance formula, as shown in Eq. (13). Next, the relationship between $E_{b,\,t}$ and SoC_t is represented in Eq. (21). Constraint (22) gives the value of the rated capacity of the battery. Constraints (23) imposes that the value of N_b should be lower than its maximum value. Finally, Eqs. (24–25) are the same as those of the generic model A. It should be noted that all variables mentioned in this work are non-negative, including $P_{\text{dis},\,t}$ and $P_{\text{out},\,t}$, although these two variables are sometimes default to take a negative sign.

C. Solution method

When the generic battery model A is used, the optimization problem, which includes Eqs. (3–12), can be written into a mixed-integer linear program, and thus the objective function can be directly optimized using standard mathematical solvers, such as `Gurobi`, which is available in many language including Python. On the other hand, if the detailed battery model B is considered, the proposed model, which corresponds to Eqs. (3–6, 13–25), is changed to be a bilinear programming problem due to the existence of the bilinear terms in Eqs. (14–17, 21). The bilinear terms present as a challenge to the optimization problem. McCormick envelopes and a bound-tightening relaxation algorithm, which have been applied to the optimization models in power systems [17], may be used to handle the bilinearity. However, the optimality of the model is *not* guaranteed. Hence, we propose next an alternative algorithm to solve the bilinear program.

It worth noting that when the integer variable N_b is fixed, the bilinear program collapses into a linear program (LP), which can then be solved by `Gurobi` easily. On this point, if the LP model is run $N_{\text{max},\,b}$ times, each corresponds to a particular N_b value, and the smallest one among the $N_{\text{max},\,b}$ number of solutions guarantees the optimality of the bilinear program; this constitutes an exhaustive search approach in terms of N_b. A clear drawback of exhaustive search is that it is time consuming. In view of that, this work proposes to replace the exhaustive search with the bisection method, which is much faster than the former while maintaining optimality. In other words, the proposed algorithm combines bisection and LP, and its pseudocode is detailed in Algorithm 1.

The bisection algorithm takes the convergence tolerance (ζ), the minimum ($N_{\text{min},\,b}$) and maximum ($N_{\text{max},\,b}$) battery numbers as inputs, and outputs the optimal battery number (N_b^*), in concert with the procedure and outcome of the LP. Before the iteration starts, the intermediate variable ($N_{\text{mid},\,b}$), which is equal to the mean of $N_{\text{min},\,b}$ and $N_{\text{max},\,b}$, is initialized on line 1. Lines 2–15 give the details of the loop. The LP solver used here is able to output two quantities, namely, the optimal objective function value, and a so-called model status variable, which indicates the convergence status of the program. In line 3, an LP model is solved when $N_b = N_{\text{mid},\,b}$, after which the objective function value (y_1) and model status (b_1) obtain. Similarly, another LP is solved in line 4 for the case of $N_b = N_{\text{mid},\,b} + 1$. It is noted that two LPs per iteration are needed, since the difference of y_1 and y_2 is used to judge the sign symbol of the derivative value at $N_{\text{mid},\,b}$. Moreover, the model status variables (b_1 and b_2) are necessary to ensure the LP solutions are unique and feasible. In other words, the algorithm completes when the model status variables take the value of "2," which, as defined by the solver, indicates an optimal solution ("1" corresponds to "loaded" and "3" corresponds to "infeasible," etc.). The algorithm terminates until the difference of $N_{\text{min},\,b}$ and $N_{\text{max},\,b}$ is lower than the convergence tolerance, while $b_1 = 2$ is true, see line 15.

Algorithm 1 bisection–LP hybrid solver

Input: the values of ζ ($\zeta > 0$), $N_{\text{min},\,b}$, and $N_{\text{max},\,b}$
Output: the optimal battery number (N_b^*)

1: initial the value for $N_{\text{mid},\,b} \leftarrow \left(N_{\text{min},\,b} + N_{\text{max},\,b}\right)/2$
2: **repeat**
3: Solve LP to obtain y_1 and b_1 for $N_b = N_{\text{mid},\,b}$
4: Solve LP to obtain y_2 and b_2 for $N_b = N_{\text{mid},\,b} + 1$
5: **if** $b_1 = 2$ **then**
6: **if** $y_1 < y_2$ **then**
7: $N_{\text{max},\,b} \leftarrow N_{\text{mid},\,b}$
8: **else if**
9: **then** $N_{\text{min},\,b} \leftarrow N_{\text{mid},\,b} + 1$
10: **end if**
11: **else if**
12: **then** $N_{\text{min},\,b} \leftarrow N_{\text{mid},\,b}$
13: **end if**
14: $N_{\text{mid},\,b} \leftarrow \left(N_{\text{min},\,b} + N_{\text{max},\,b}\right)/2$
15: **until** ($N_{\text{max},\,b} - N_{\text{min},\,b} <= \zeta$ and $b_1 = 2$)

III. Physical Model Chain for PV Power Modeling

Firm power delivery can be realized on both existing the PV plant and new PV plant. In the case of the former, one needs to expand the original installed capacity according to the historical power measurements collected on-site. However, during the planning and design of a new firm PV plant, historical data is not available, and one must simulate the PV power output via, e.g., satellite-derived irradiance data and energy meteorology models [18]. Converting satellite-derived irradiance (and other auxiliary variables such as air temperature and wind speed) to PV power is not a trivial task, for it involves a sequence of models, each established upon intricate scientific or engineering principles, see [19–21] for discussions. Since these models are used in cascade, where the output of one model is the input of another, this framework

of irradiance-to-power conversion is called the model chain. Figure 3 shows the schematic of the simplified model chain used in this work.

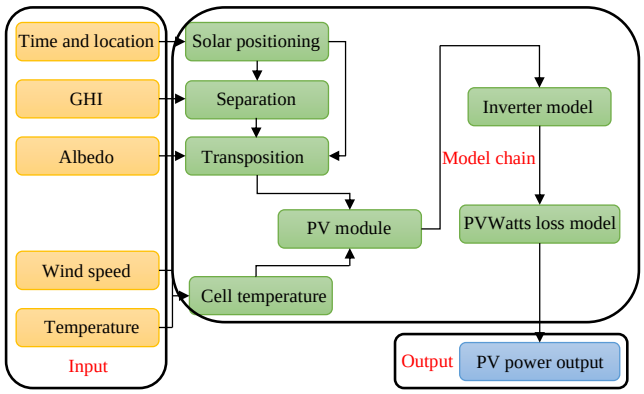

Fig. 3. A schematic diagram of a basic model chain, which utilizes global horizontal irradiance (GHI), albedo, wind speed, temperature, time, and location as inputs, and yields the PV power.

The input of this model chain consists of five elements. First, time and location information is used to compute the angles describing the sun's position relative to observers on both horizontal and tilted surfaces; this stage is known as solar positioning. Several algorithms are available, and among them, there is a general trade-off between computation speed and accuracy. Since speed is not a concern for the present simulation, the algorithm of Reda and Andreas [22] is herein used, which is the most accurate one to date. Solar positioning yields the zenith angle (Z) and incidence angle (θ), which are required by separation and transposition models.

In separation modeling, global horizontal irradiance (GHI) is split into a beam component and a diffuse component based on the closure relationship:

$$G_h = B_h + D_h = B_n \cos Z + D_h, \tag{26}$$

where G_h, B_h, and D_h are GHI, beam horizontal irradiance (BHI), and diffuse horizontal irradiance (DHI), respectively; B_n is the beam normal irradiance, which differs from B_h by a factor of cosine of zenith. Hundreds of separation models have been proposed in the literature, and their performance is inhomogeneous across geographical locations, time periods, and sky conditions [23]. For instance, a rational strategy is to treat clear- and cloudy-sky conditions separately, which is also the approach adopted here. For clear-sky conditions, the REST2 model [24] directly estimates the clear-sky beam and diffuse components, whereas for cloudy-sky conditions, the DISC model [25] is used.

With the estimated B_n and D_h, the transposition model converts the horizontal irradiance components to the global tilted irradiance (GTI):

$$G_c = B_n \cos\theta + R_d D_h + \rho R_r G_h, \tag{27}$$

where G_c is the GTI on the tilted collector surface; $R_r = (1 - \cos S)/2$ is the transposition factor due to ground reflection, where S is the PV tilt; ρ is the foreground's albedo, which can be obtained through either measurement or remote sensing; and R_d is the diffuse transposition factor, which can be estimated via different options [26]. Among the many options, the 1990 version of the Perez model [27] is widely regarded as the most accurate one, it is therefore used in this paper. More specifically, the Perez model states:

$$R_d = (1 - F_1)\frac{1 + \cos S}{2} + F_1 \frac{\max(0, \cos\theta)}{\max(0.087, \cos Z)} + F_2 \sin S, \tag{28}$$

where F_1 and F_2 are sky-condition-dependent parameters that can be looked up from Tables 1 and 6 of [27].

Whereas GTI is the most influential factor affecting the PV output, the cell temperature (T_{cell}) is the next-important one. Estimating cell temperature is known *a priori* to be linked to ambient temperature. Besides that, heat removal through convection reduces cell temperature, and thus wind (mostly wind speed, and to some extent, wind direction) is also taken to be a second-order variable during cell-temperature modeling. Similar to the previous stages in the model chain, there are numerous available cell temperature models. Without loss of generality, the Sandia model [28] is considered here:

$$T_{\text{cell}} = T_{\text{mod}} + \frac{G_c}{1000\ \text{W/m}^2}\Delta T, \tag{29}$$

$$T_{\text{mod}} = G_c \exp(p + qV) + T_{\text{amb}}, \tag{30}$$

where T_{mod} and T_{amb} are module and ambient temperature, respectively; V is wind speed; ΔT, p and q are empirical coefficients for the different encapsulation–mounting combinations. For example, for glass/polymer modules with open-rack mounting, $\Delta T = 3°\text{C}$, $p = -3.56$, and $q = -0.075$.

PV models, which convert GTI, cell temperature, and other PV system design parameters into DC output, can be classified into two types [19]. Empirical models form one category, whereas those that adopt physical modeling of an equivalent circuit form the other. Physical models are able to trace out the entire I–V curve of the system, but require system design to be known. In contrast, empirical models do note require that and can offer acceptable accuracy. In this work, the empirical PVWatts model [29] is used:

$$P_{\text{dc}} = P_s \frac{G_c}{1000\ \text{W/m}^2}\left[1 + \gamma_{\text{ref}}\left(T_{\text{cell}} - 25°\text{C}\right)\right], \tag{31}$$

where P_{dc} is the DC power output of the PV plant, and γ_{ref} is the temperature coefficient of the rated power of the PV modules with a unit of $\%/°\text{C}$.

Before injection to the grid, DC power needs to be converted to AC power. With the input of the DC power calculated by the preceding part of the model chain, the PVWatts inverter model [29] is taken for DC–AC conversion:

$$\eta_{\text{inv}} = \frac{\eta_{\text{norm}}}{\eta_{\text{ref}}}\left(-0.0162\varsigma - \frac{0.0059}{\varsigma} + 0.9858\right), \tag{32}$$

$$P_{\text{ac}} = \min\left(\eta P_{\text{dc}}, P_{\text{ac,ref}}\right), c \tag{33}$$

where $\eta_{\text{inv}} = P_{\text{dc}}/P_{\text{dc,ref}}$, $P_{\text{dc,ref}} = P_{\text{ac,ref}}/\eta_{\text{norm}}$, η_{inv} is the actual inverter efficiency, η_{norm} is the nominal inverter efficiency, η_{ref} is the reference inverter efficiency, $P_{\text{dc,ref}}$ and $P_{\text{ac,ref}}$ are respectively the DC power input limit and AC power output limit of the inverter, and P_{ac} is the AC output of the

PV plant. It is worth mentioning that any AC power exceeding $P_{\text{ac, ref}}$ is truncated, of which the action is known as inverter clipping.

At this stage, the AC power output has been acquired. Nevertheless, to simulate PV power in a more realistic way, one still needs to factor in various losses, such as snow loss, wiring loss, or shading loss. Modeling physical losses exactly also requires design information, and the outcome is not always superior to simple empirical approaches. Hence, the PVWatts loss model [29] is considered to lump the various losses.

IV. A Case Study on Firm Generation

A. Case Study Parameters

The principle of firm power delivery and model chain construction described in the previous two sections are general, and can be applied to any location insofar as the solar resource data, modeling parameters, and load profiles are available. Without loss of generality, the firm PV plant is assumed to be situated in Harbin (45.76° N, 126.64° E), China. The DC rated power (P_s) is set to be 1 MW. The firm PV plant is intended to serve a 0.17-MW constant load all year round. This constant load is chosen for not just simplicity but also its ability to conservatively isolate the effect of the load profile on the results. Employing the physical model chain, the power output ($P_{\text{pv}, t}$) of the firm PV plant is simulated with the TMY dataset downloaded from National Solar Radiation Database (NSRDB) [30]. TMY, which is composed of individual monthly data from different years each characterizing the median weather condition of the month, is ubiquitously used in solar engineering, design, and bankability studies. However, it should be noted that when actual load profile is used in concert with TMY dataset, the time synchronization between the two must be ensured, i.e., for each TMY month, the same-month load data must be used.

TABLE I
Parameter Setting of the Case Study.

Par.	Value	Source	Par.	Value	Source
c_b	137 \$/kWh	[31]	c_s	833 \$/kW	[32]
l_b	0.02%	[8]	l_s	1%	[8]
$N_{\text{max}, b}$	20 000	–	$N_{\text{min}, b}$	0	–
$P_{\text{ac, ref}}$	0.833 MW	[33]	p	−3.56	[28]
q	−0.075	[28]	S	45.76°	–
$S_{b, \text{ref}}$	5.32 kWh	[34]	T_b	15 years	[35]
T_s	30 years	[35]	ε_b	95%	[21]
ζ	1	–	η_{norm}	97.5%	[33]
η_{ref}	96.37%	[29]	γ_{ref}	−0.45%/°C	[33]
σ_b	0.01%	[21]	τ	8%	[21]
Δt	1 hour	–	ΔT	3°C	[28]

With the location and unconstrained PV capacity fixed, the basic PV plant design information needs to be sought. To do so, we solicit different parameter values from various credible sources, see Table I. For instance, following the conventional wisdom, a DC/AC ratio of 1.2 is used, which implies an AC rated power ($P_{\text{ac, ref}}$) of 0.833 MW. The nominal inverter efficiency (η_{norm}) is 97.5% [33], and the reference inverter efficiency (η_{ref}) is 96.37% [29]. The temperature coefficient of the rated power of the PV modules (γ_{ref}) is taken to be $-0.45\%/°\text{C}$. As for losses, the default values for soiling loss, snow loss, wiring loss, and other losses are assumed to be 2%, 3%, 2%, and 3%, respectively. The irradiance-to-power conversion is implemented in the open-source `pvlib-python` package [33], from which the details of the selected PV modules and inverter can also be retrieved.

Besides the parameters used for model chain, one also has to set the parameters of the optimization model for the firm kWh premium estimation, see Table I. From Statista, it is sourced that the average investment cost per kW (c_s) of the PV plant was 883 \$/kW worldwide in 2020 [32], and the average investment cost per kWh (c_b) of lithium battery storage worldwide was 137 \$/kWh in the same year [31]. Based on [35], the lifetime of PV (T_s) and battery (T_b) are respectively set to be 30 and 15 years. If battery storage was charged at the maximum power, it is assumed that it would take 4 h to go from empty to the full-charge state, namely, $P_{\text{ch, max}} \times 4 \text{ h} = S_b$. The same rule is applied to $P_{\text{dis, max}}$. Consistent with [21], a conservative discount rate (τ) of 8% is used, the self-discharge rate (σ_b) is taken to be 0.01%, and the charging/discharging efficiency (ε_b) is 95%. The O&M cost factor (l_s) is 1.0% for the PV plant on a yearly basis and 0.02% for battery storage (l_b) per full charge cycle, following [8]. Besides, the actual charging/discharging sampled points used by Ref. [34] come from a battery storage with a rated capacity ($S_{b, \text{ref}}$) of 5.32 kWh. In the bisection algorithm, the minimum ($N_{\text{min}, b}$) and maximum ($N_{\text{max}, b}$) battery numbers are respectively set as 0 and 20 000 (i.e., the highest battery capacity is 106.4 MWh), wheres the convergence tolerance (ζ) is one (i.e., batteries are discrete).

B. Optimization results

Results using battery model A: Recalling the objective function (3), in principle, both the oversizing ratio X_s and the rated capacity of battery storage S_b, as well as the intermediate variables such as $P_{\text{ch}, t}$ can be optimized simultaneously when the generic battery model A is employed. For investigation purposes, however, one may wish to examine the variation of the firm kWh premium with the oversizing ratio. In such situations, it is possible to fix X_s at a range of values, e.g., $\{1, 1.01, \ldots, 10\}$ with a step size of 0.01, and optimize S_b for each X_s value. In any case, once with X_s and S_b found, the optimal firm kWh premium can be calculated via Eqs. (1) and (2) after considering the annual solar energy yield and annual constant load. Figure 4 (A) illustrates the value of the firm kWh premium for the PV system of concern as a function of X_s when the battery constrains are Eqs. (7–12); the contributions from the PV plant and battery storage are broken down for visualization.

It is evident from Fig. 4 (A) that, when $X_s = 1$, i.e., no oversizing, an exceedingly high firm kWh premium of 20.49 is required to firm up the generation. However, with just a small fraction of overbuilding, there is a drastic decrease in the firm kWh premium—when $X_s = 1.77$, the firm kWh premium sees a five-fold reduction, reaching just 4.18. As more PV is overbuilt, the premium starts to increase quasi-linearly. These

observations can be explained as follows: To firmly meet the 0.17-MW constant load, the duration and magnitude of the load–supply mismatch sharply collapses (cf. Fig. 1) and then saturates with further increasing X_s. Consequently, one can conclude that the saved cost of excess battery storage can well cover the additional cost of PV overbuilding, as to reach an optimal combined use of the two firm power enablers. To summarize, the least cost of firm PV power under the current simulation setup in the case using the simple battery model A can be achieved with an additional 0.77 MW PV overbuilding and a battery storage with a rated capacity of 8.85 MWh.

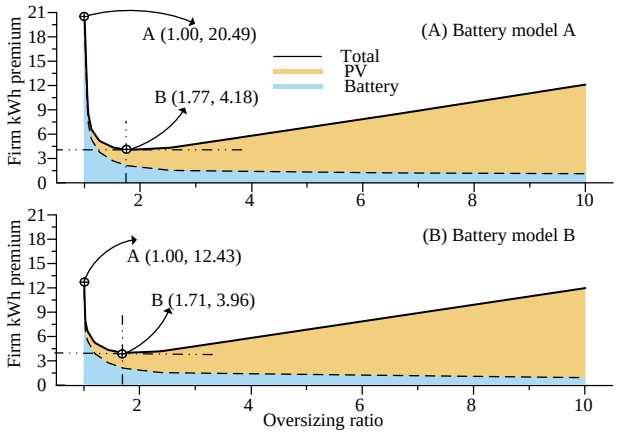

Fig. 4. Firm kWh premium of the PV system of concern as a function of the PV oversizing ratio in cases using the generic battery model A (top) and measurement-based battery model B (bottom). The blue and orange areas mark the cost contributions from battery and PV, respectively. When firm power is delivered via a battery-only solution, its firm kWh premium is high (point A in figure). In contrast, when an optimized multiplier of PV is overbuilt, the firm kWh premium drops to a nadir value (point B), owing to the substantially smaller battery. As the PV oversizing ratio increases further, the firm kWh premium rises quasi-linearly due to effects of diminishing returns.

Result comparison under the two battery models: As can be observed from Fig. 4, the variation pattern of the firm kWh premium of the PV system with respect to the PV oversizing ratio under the scenario using the simple battery model A is nearly the same as that in the case using a more realistic battery model B. Particularly, the optimal firm kWh premium for the former model is 4.18, whereas the corresponding value is 3.96 for the latter model. This shows that the high intricacy of the battery model does not alter the firm kWh premium much, since the difference between the two optimal values is only 0.22. Regarding the higher value of the optimal firm kWh premium in the case with generic battery model, it may be due to an over-pessimistic assumption about the battery charging/discharging efficiency. More specifically, a constant battery efficiency of 0.95 is assumed for battery model A, whereas the average charging and discharging efficiencies calculated empirically from the real operation profiles are 0.99 for the measurement-based battery model B. The main reason why the efficiency of the battery model B is nearly close to one is that the values of the SoC of the battery are almost always above 0.05, as shown in Fig. 5 (B), which avoids the low-efficiency charging/discharging behaviors. Figure 5 also shows that there are not many hours when the SoC values of the battery exceed 0.5 for both battery models. If battery activities during these periods are replaced by the existing dispatchable units such as gas turbines, the rated capacity of the battery could be halved, which would further reduce the above optimal firm kWh premium. In the following subsections, although battery model B can characterize the battery performance more accurately than battery model A, only model A is used, since there is only a marginal difference in firm kWh premiums calculated by the two battery models.

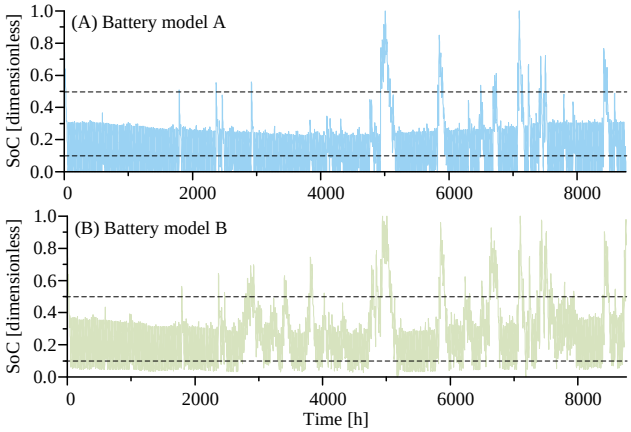

Fig. 5. State of charge of the battery: (A) generic battery model A, and (B) measurement-based battery model B.

C. Influence of the choice of the model chain on firm kWh premium

The PV power output in this work is simulated using the physical model chain, which consists of disparate component models, each with numerous variants. That is to say, even with the same weather inputs, diverse PV generation behaviors might be observed if different model chains are selected. In this regard, the impact of the choice of the model chain on the firm kWh premium is demonstrated here. Note that separation model and transposition model are the two most essential steps in model chain [19], and separation model can be skipped in this work since the weather dataset already contains GHI, BHI, and DHI. Consequently, we only consider model chains with different options of transposition models, with other component models remain the same as described in Section III. Five transposition models, namely, King model, Reindl's 1990 model, Klucher's 1979 model, Hay & Davies's 1980 model, and Perez's 1990 model [33], are considered. The results on the calculated firm kWh premium are listed in Table II.

Evidently, there are differences in the results. However, the gap between the highest and lowest firm kWh premium values is only 1.67%, and that between the highest and lowest annual PV productions is 1.64, which are both negligible in view of other larger sources of uncertainties, such as the interannual variability in solar resource, see below. Therefore, the choice of transposition models does not incur significant differences on the firm kWh premium and annual solar energy yield. From this finding, one may further infer that the choice of model

TABLE II
FIRM KWH PREMIUM AND ANNUAL PV PRODUCTION OF THE PV SYSTEM OF INTEREST UNDER FIVE VARIANTS OF TRANSPOSITION MODELS, EACH WITH A DIFFERENT SKY DIFFUSE IRRADIANCE MODEL.

Sky diffuse irradiance models	Firm kWh premium	Annual PV production (MWh)
King model	4.12	1638
Reindl's 1990 model	4.15	1620
Klucher's 1979 model	4.12	1616
Hay & Davies's 1980 model	4.15	1611
Perez model	4.18	1636

chain is not a sizable source of uncertainty in firm power delivery optimization.

D. Sensitivity of the Firm kWh Premium to Solar and Battery Costs

The firm kWh premium can be considered as the cost multiplier to firm up PV generation with respect to the cost of unconstrained PV. Although the optimal firm kWh premium of 4.18 under the current PV–battery price structure is already substantially lower than that of the battery-only solution, which is 20.49, this 4x multiplier in cost is still not acceptable, for the PV plant owners need to quadruple their total investment. Currently, unconstrained PV has reached grid parity in many parts of the world, but firm PV would again make solar a less competitive option than conventional thermal generation. Hence, this section investigates how future price trends of PV and battery can affect the firm kWh premium and LCOE, and whether or not *true* grid parity of PV can be eventually achieved. In this regard, a sensitivity analysis on the firm kWh premium and LCOE in response to the unit investment costs of battery storage (c_b) and PV (c_s) is conducted. More specifically, c_b is selected from the set of $\{20, 30, \ldots, 180\}$ in steps of 10 \$/kWh, whereas c_s is drawn from the set $\{100, 120, \ldots, 1000\}$ in steps of 20 \$/kW. Our choice takes regular intervals on the prices, from their current levels (833 \$/kW for PV and 137 \$/kWh for battery, which have been provided in Section IV), to some ideally low levels (100 \$/kW for PV and 20 \$/kWh for battery), in that, the considered scenarios are designed to cover "all" possible scenarios [36, 37]. Figure 6 plots the heat maps of the optimal firm kWh premium and LCOE of firm PV for different pairs of c_s and c_b values.

From Fig. 6 (A) one can observe that the lowest firm kWh premium occurs when the PV cost is high and battery cost is low—with $c_s = 1000$ \$/kW and $c_b = 20$ \$/kWh, the premium is just 1.88. This low value stems from how the firm kWh premium is defined: The more expensive PV is relative to battery, the smaller relative cost is needed to firm up generation. That said, the real insights come from Fig. 6 (B), where the reduction of LCOE is evident with a decrease in either c_s or c_b. The red line in the figure marks the current average feed-in tariff of China, which is 5.10 ¢/kWh [38, 39]. If the LCOE of firm PV falls below that number, firm PV becomes truly competitive. The LCOE of firm PV at present day is 21.65 ¢/kWh, which is 4.2 times that of the average feed-in tariff. To reach below 5.10 ¢/kWh, and based on the simulation, one requires a combination of $c_s < 250$ \$/kW and $c_b < 40$ \$/kWh. The differences between the current and future prices of PV and battery are to be narrowed by technological advancements and radical changes in energy policies.

E. Effects of Inter-annual Variability on the Firm kWh Premium

The analysis on the firm kWh premium is conducted thus far with the TMY dataset. Since TMY is a dataset that portrays the most typical weather regime of a location, the corresponding results can also be regarded as typical. Notwithstanding, it is well known that solar resource exhibits inter-annual variability, in that, resource availability varies somewhat from one year to another. Hence, to ensure the long-term validity of firm power delivery, one has to consider not just the typical scenario but also the worst-case scenario. On this point, the optimization of the firm kWh premium is repeated with weather data from each individual year during a ten-year (2011–2020) period. In other words, this section seeks to examine the robustness of firm power delivery. The result is shown in Fig. 7.

It can be seen from Fig. 7 that the firm kWh premium computed using the TMY dataset is in fact lower than that of most individual years. This result can be easily understood, as the TMY dataset does not contain those small-probability prolonged low-resource periods, which can drive up the premium significantly. For instance, over this 10-year period, the highest premium of 6.87 takes place in 2013, which is much higher than the TMY premium of 4.18. What this case study reveals is that if we are to design a firm power plant based just on TMY data, it is very likely that the designed plant fails to meet the firm power delivery requirement in practice. This finding is contradictory to the current industrial practice where TMY is acceptable and thus universally used for plant design and bankability studies. Rather, the design of the firm power plant should not rely on TMY, but the worst-case scenario, which can only be realized if long-term weather data is available. In a more general sense, when actual load is in use, the worst-case scenario corresponds, for example, to highest-load–lowest-resource months/year. However, since such worst-case scenario occur rather infrequently over the lifetime of the firm PV system, it may be more economic to engage other failsafe devices as opposed to overbuilding more PV and/or installing more batteries.

To put this inter-annual concern in a practical operational perspective, the concept of supply-side flexibility has been introduced and applied by Perez et al. [10]. Supply-side flexibility assumes that a small fraction (typically $< 5\%$) of electrical demand is met by conventional thermal generation, thereby removing extreme event contingencies. Flexible power such as that from spinning reserve is applied any time when storage runs out. In a recent investigation Remund et al. [40] showed that even if very expensive 100% renewable e-fuels are used in lieu of standard natural gas to power thermal generation, the impact on the bottom-line electricity cost is negligible, while the impact on the bottom-line premium can be far reaching, removing extreme overbuild/storage contingencies.

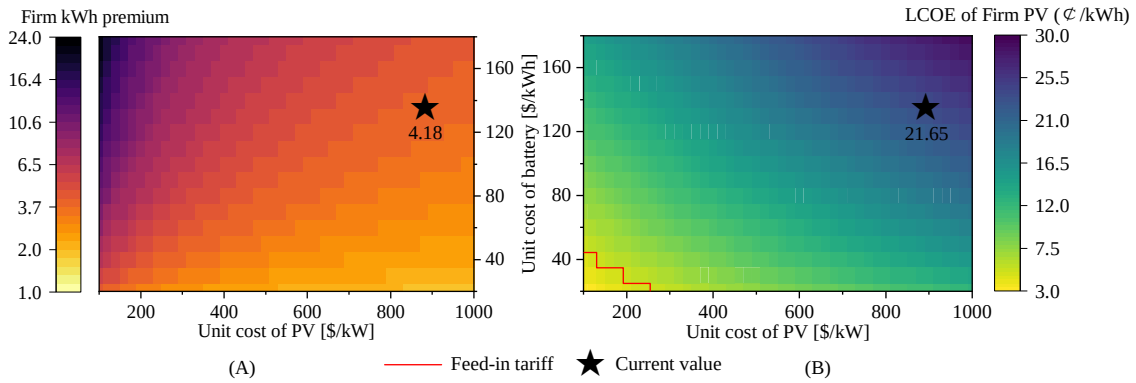

Fig. 6. Heat maps of (A) the firm kWh premium and (B) LCOE of the firm PV, as functions of PV and battery costs. The black star in each panel represents the scenario under current PV and battery costs (Section IV-B), that is, c_s = 883 \$/kW and c_b = 137 \$/kWh. The red solid line in (B) marks the average feed-in tariff of 5.10 ¢/kWh in China in 2019, which is sourced from [38, 39].

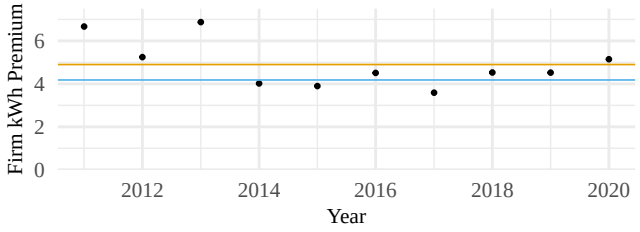

Fig. 7. Firm kWh premium of the PV system of concern over a period of 10 years (2011–2020). The two horizontal lines indicate the 10-year-average premium (orange) and the premium calculated from the TMY dataset (blue).

V. Conclusion

Intermittency, variability, and the non-dispatchable nature present the greatest challenges in matching the properties of solar PV power to convention thermal power. Firm power enablers, which are technologies that can help PV power to meet the targeted load with 100% certainty, are of great interest. Among various enablers, the combination of battery storage and PV overbuilding seems particularly attractive, in that, they are neither passive as geographical smoothing is, nor to they require consumers to change their electricity consumption as in demand response.

Although firm power delivery has been studied previously, this paper proposes a new mathematical optimization model for calculating the firm kWh premium, which is an indicator of the cost-effectiveness of firm power enablers. To characterize the operation behaviors of the battery, two models are considered, one generic and the other detailed, which render the aforementioned optimization model either a mixed-integer linear program or a bilinear program. Since the bilinear problem is hard to solve, an alternative algorithm is presented to ensure optimality. Besides, the effects and implications on the firm kWh premium due to (1) future price trends of PV and battery, (2) the choice of model chain, and (3) inter-annual variability in solar resources, are analyzed and investigated.

From the optimization results, it is found that the lowest firm kWh premium under the present-day cost structure at the selected northern China location is around 4.18 when the generic battery model is employed. Despite the five-fold reduction as compared to the premium of a battery-only solution, this value is still too high for firm PV to be considered as truly competitive in electricity markets. Besides, granularity in battery modeling and the choice of the model chain are found to have only a marginal effect on the firm kWh premium. To drop the LCOE of firm PV below grid parity, the unit investment costs of PV and battery need to be lower than 250 \$/kW and 40 \$/kWh, respectively. The practice of using TMY dataset to analyze the firm kWh premium, as it is used ubiquitously for standard solar resource assessment and bankability studies, is found inadequate, since it does not contain the worst-case weather scenario for strictly 100% PV applications. To remedy the situation, historical weather data over a long period of time such as a decade is thought essential to arrive at an accurate estimate of the firm kWh premium. In practice, however, a small amount of supply-side flexibility can lead to economically acceptable 100% renewable firm power operations.

References

[1] Y. S. Perdana, S. M. Muyeen, A. Al-Durra, H. K. Morales-Paredes, and M. G. Simões, "Direct connection of supercapacitor–battery hybrid storage system to the grid-tied photovoltaic system," *IEEE Transactions on Sustainable Energy*, vol. 10, no. 3, pp. 1370–1379, 2019.

[2] X. Li, D. Hui, and X. Lai, "Battery energy storage station (BESS)-based smoothing control of photovoltaic (PV) and wind power generation fluctuations," *IEEE Transactions on Sustainable Energy*, vol. 4, no. 2, pp. 464–473, 2013.

[3] M. Lave, J. Kleissl, and J. S. Stein, "A wavelet-based variability model (WVM) for solar PV power plants," *IEEE Transactions on Sustainable Energy*, vol. 4, no. 2, pp. 501–509, 2013.

[4] V. Walter and L. Göransson, "Trade as a variation management strategy for wind and solar power integration," *Energy*, vol. 238, p. 121465, 2022.

[5] Y. Li, M. Han, Z. Yang, and G. Li, "Coordinating flexible demand response and renewable uncertainties for scheduling of community integrated energy systems with an electric vehicle charging station: A bi-level approach," *IEEE Transactions on Sustainable Energy*, vol. 12, no. 4, pp. 2321–2331, 2021.

[6] N. Mahdavi, J. H. Braslavsky, M. M. Seron, and S. R. West, "Model predictive control of distributed air-conditioning loads to compensate fluctuations in solar power," *IEEE Transactions on Smart Grid*, vol. 8, no. 6, pp. 3055–3065, 2017.

[7] R. Perez, K. R. Rábago, M. Trahan, L. Rawlings, B. Norris, T. Hoff, M. Putnam, and M. Perez, "Achieving very high PV penetration – The need for an effective electricity remuneration framework and a central role for grid operators," *Energy Policy*, vol. 96, pp. 27–35, 2016.

[8] M. Perez, R. Perez, K. R. Rábago, and M. Putnam, "Overbuilding & curtailment: The cost-effective enablers of firm PV generation," *Solar Energy*, vol. 180, pp. 412–422, 2019.

[9] M. J. Perez, R. Perez, and T. E. Hoff, "Ultra-high photovoltaic penetration: Where to deploy," *Solar Energy*, vol. 224, pp. 1079–1098, 2021.

[10] R. Perez, M. Perez, J. Schlemmer, J. Dise, T. E. Hoff, A. Swierc, P. Keelin, M. Pierro, and C. Cornaro, "From firm solar power forecasts to firm solar power generation an effective path to ultra-high renewable penetration a New York case study," *Energies*, vol. 13, no. 17, p. 4489, 2020.

[11] R. Perez, M. Perez, M. Pierro, J. Schlemmer, S. Kivalov, J. Dise, P. Keelin, M. Grammatico, A. Swierc, J. Ferreira, A. Foster, M. Putnam, and T. Hoff, "Operationally perfect solar power forecasts: A scalable strategy to lowest-cost firm solar power generation," in *2019 IEEE 46th Photovoltaic Specialists Conference (PVSC)*, vol. 2, 2019, pp. 1–6.

[12] M. Perez, "A model for optimizing the combination of solar electricity generation, supply curtailment, transmission and storage," Ph.D. dissertation, Columbia University, 2014.

[13] R. Sioshansi, P. Denholm, J. Arteaga, S. Awara, S. Bhattacharjee, A. Botterud, W. Cole, A. Cortés, A. d. Queiroz, J. DeCarolis, Z. Ding, N. DiOrio, Y. Dvorkin, U. Helman, J. X. Johnson, I. Konstantelos, T. Mai, H. Pandžić, D. Sodano, G. Stephen, A. Svoboda, H. Zareipour, and Z. Zhang, "Energy-storage modeling: State-of-the-Art and future research directions," *IEEE Transactions on Power Systems*, vol. 37, no. 2, pp. 860–875, 2022.

[14] A. V. Vykhodtsev, D. Jang, Q. Wang, W. Rosehart, and H. Zareipour, "Linearized physics-based Lithium-ion battery model for power system economic studies," *arXiv preprint arXiv:2207.03469*, 2022.

[15] A. J. Gonzalez-Castellanos, D. Pozo, and A. Bischi, "Non-ideal linear operation model for Li-ion batteries," *IEEE Transactions on Power Systems*, vol. 35, no. 1, pp. 672–682, 2020.

[16] K. Antoniadou-Plytaria, D. Steen, L. A. Tuan, O. Carlson, B. Mohandes, and M. A. F. Ghazvini, "Scenario-based stochastic optimization for energy and flexibility dispatch of a microgrid," *IEEE Transactions on Smart Grid*, vol. 13, no. 5, pp. 3328–3341, 2022.

[17] S. Chen, A. J. Conejo, R. Sioshansi, and Z. Wei, "Unit commitment with an enhanced natural gas-flow model," *IEEE Transactions on Power Systems*, vol. 34, no. 5, pp. 3729–3738, 2019.

[18] D. Yang, W. Wang, and X. Xia, "A concise overview on solar resource assessment and forecasting," *Advances in Atmospheric Sciences*, vol. 39, no. 8, pp. 1239–1251, 2022.

[19] M. J. Mayer and G. Gróf, "Extensive comparison of physical models for photovoltaic power forecasting," *Applied Energy*, vol. 283, p. 116239, 2021.

[20] M. J. Mayer, "Benefits of physical and machine learning hybridization for photovoltaic power forecasting," *Renewable and Sustainable Energy Reviews*, vol. 168, p. 112772, 2022.

[21] W. Wang, D. Yang, N. Huang, C. Lyu, G. Zhang, and X. Han, "Irradiance-to-power conversion based on physical model chain: An application on the optimal configuration of multi-energy microgrid in cold climate," *Renewable and Sustainable Energy Reviews*, vol. 161, p. 112356, 2022.

[22] I. Reda and A. Andreas, "Solar position algorithm for solar radiation applications," *Solar Energy*, vol. 76, no. 5, pp. 577–589, 2004.

[23] D. Yang, "Estimating 1-min beam and diffuse irradiance from the global irradiance: A review and an extensive worldwide comparison of latest separation models at 126 stations," *Renewable and Sustainable Energy Reviews*, vol. 159, p. 112195, 2022.

[24] C. A. Gueymard, "REST2: High-performance solar radiation model for cloudless-sky irradiance, illuminance, and photosynthetically active radiation – Validation with a benchmark dataset," *Solar Energy*, vol. 82, no. 3, pp. 272–285, 2008.

[25] E. L. Maxwell, "A quasi-physical model for converting hourly global horizontal to direct normal insolation," Solar Energy Research Inst., Golden, CO (USA), Tech. Rep. SERI/TR-215-3087, 1987.

[26] D. Yang, "Solar radiation on inclined surfaces: Corrections and benchmarks," *Solar Energy*, vol. 136, pp. 288–302, 2016.

[27] R. Perez, P. Ineichen, R. Seals, J. Michalsky, and R. Stewart, "Modeling daylight availability and irradiance components from direct and global irradiance," *Solar Energy*, vol. 44, no. 5, pp. 271–289, 1990.

[28] D. L. King, J. A. Kratochvil, and W. E. Boyson, "Photovoltaic array performance model," Sandia National Laboratories, Albuquerque, NM (United States), Tech. Rep. SAND2004-3535, 2004.

[29] A. P. Dobos, "Pvwatts version 5 manual," National Renewable Energy Lab. (NREL), Golden, CO (United States), Tech. Rep., 2014.

[30] M. Sengupta, Y. Xie, A. Lopez, A. Habte, G. Maclaurin, and J. Shelby, "The National Solar Radiation Data Base (NSRDB)," *Renewable and Sustainable Energy Reviews*, vol. 89, pp. 51–60, 2018.

[31] M. Placek. Lithium-ion battery pack costs worldwide between 2011 and 2030. (2022, June 17). [Online]. Available: https://www.statista.com/statistics/883118/global-lithium-ion-battery-pack-costs/.

[32] M. Jaganmohan. Average installed cost for solar photovoltaics worldwide from 2010 to 2020. (2022, June 17). [Online]. Available: https://www.statista.com/statistics/809796/global-solar-power-installation-cost-per-kilowatt/.

[33] W. F. Holmgren, C. W. Hansen, and M. A. Mikofski, "pvlib python: A python package for modeling solar energy systems," *Journal of Open Source Software*, vol. 3, no. 29, p. 884, 2018.

[34] A. J. Gonzalez-Castellanos, D. Pozo, and A. Bischi. Data for: A detailed Li-ion battery operation model, version 1. (2023, February 13). [Online]. Available: https://data.mendeley.com/datasets/36w7ts3r4t.

[35] W. J. Cole, A. Frazier, P. Donohoo-Vallett, T. T. Mai, and P. Das, "2018 standard scenarios report: A U.S. electricity sector outlook," National Renewable Energy Lab. (NREL), Golden, CO (United States), Tech. Rep., 2018.

[36] International Renewable Energy Agency. Future of Solar Photovoltaic: Deployment, investment, technology, grid integration and socio-economic aspects. (2023, February 13). [Online]. Available: https://www.irena.org/-/media/Files/IRENA/Agency/Publication/2019/Nov/IRENA_Future_of_Solar_PV_2019.pdf.

[37] L. Mauler, F. Duffner, W. G. Zeier, and J. Leker, "Battery cost forecasting: a review of methods and results with an outlook to 2050," *Energy & Environmental Science*, vol. 14, no. 9, pp. 4712–4739, 2021.

[38] State Grid Corporation of China. International comparative analysis for the electricity prices of China. (2023, February 13). [Online]. Available: http://www.sasac.gov.cn/n16582853/n16582883/c17715327/content.html.

[39] State Administration of Foreign Exchange. Table of the exchange rate of various currencies against to the US Dollar (2019, December 31). (2023, February 13). [Online]. Available: http://m.safe.gov.cn/safe/2019/1231/15022.html.

[40] J. Remund, R. Perez, and M. Perez, "Firm PV power generation for Switzerland," Swiss Federal Office of Energy SFOE, Tech. Rep. SI/502286-01, 2022.